15TH IEA HEAT PUMP CONFERENCE
MAY 26–29, 2026 | HOFBURG
VIENNA 2026
DECARBONISATION THROUGH INNOVATION

Numerical investigation of liquid injection and bearing leakage in industrial heat pumps

Robin Tassenoy[a,*], Elias Vieren[a], Thibault Huyghe[a], Jari Raeymackers[a], Kenny Couvreur[a], Tim Van Craeynest[a], Michel De Paepe[a,b,c], Steven Lecompte[a,b]

[a]Ghent University, Department of Electromechanical, Systems and Metal Engineering, Sint-Pietersnieuwstraat 41, Ghent 9000, Belgium
[b]FlandersMake@UGent, Core lab MIRO, Gaston Geenslaan 8, Heverlee 3001, Belgium
[c]University of Cape Town, Department of Mechanical Engineering, Private Bag X3, Rondebosch 7701, South Africa

Abstract

Process heating accounts for 53.5% of the total industrial energy demand, and thus contributes significantly to industrial greenhouse gas emissions. 37% of this heat demand is required at temperatures below 200 °C, which means high-temperature heat pumps (HTHPs) have significant decarbonization potential. These heat pumps have been demonstrated up to 160 °C, but are available up to 200 °C only as concept or at lab scale. Recently, natural refrigerants are favoured to synthetic ones as they are more environmentally friendly. A 30 kWe HTHP demonstrator using water-ammonia mixture as refrigerant is currently being commissioned at Ghent University. It is designed to heat up oil to 200 °C. The demonstrator is equipped with refrigerant injection to avoid excessively high compressor discharge temperatures. Moreover, it uses an oil-free twin-screw compressor. The hydrodynamic bearings are lubricated using the refrigerant mixture itself, meaning bearing leakage provides additional cooling effect. This contribution presents a dynamic model of this experimental setup to study the system performance and control strategy. In particular, the optimization of the liquid injection and bearing lubrication loop pressure are addressed, and the potential impact of the currently unknown bearing leakage is studied to support the commissioning efforts. The study shows that liquid injection effectively limits the compressor discharge temperature when adequately controlled. The lubrication loop pressure on the other hand has negligible impact on the system operation and is thus not a priority during commissioning. Finally, it is shown that limited bearing leakage can benefit the heat pump performance, as long it does not become excessive.

Keywords: High-temperature heat pump; water; ammonia; injection; model ;

1. Introduction

Industrial energy demand contributes 24.2% of the greenhouse gas emissions worldwide [1]. Thermal energy represents 81 % of the total industrial energy demand in Europe, with 66 % specifically used for process heating [2]. Noticeably, 37% of this process heating is required at temperatures below 200 °C [2]. Industrial process heat up to 200 °C thus accounts for about one fifth of the final European industrial energy demand.

To decarbonize this heat, several high temperature heat pumps (HTHPs) are commercialized, or in the process of being commercialized, with a strong focus on closed-cycle vapour compression heat pumps. HTHPs with delivery temperatures up to 120 °C are commercially rolled out. For higher supply temperatures between 120 and 160 °C demonstration units are being installed and tested. However, the technology is at prototype stage for temperatures above 160 °C [3].

* Corresponding author. Tel.: +32 9 264 33 59
E-mail address: Robin.Tassenoy@UGent.be

Given the industrial heat demand, heat pumps up to 200 °C represent a significant decarbonization potential. While several commercial high-temperature heat pumps use synthetic refrigerants, natural refrigerants regained interest as they are more environmentally friendly. R-744 (CO_2) and hydrocarbons are mostly used for delivery temperatures above 95 °C. Despite the promising characteristics of R-744, it is only suitable for industrial heating processes with substantial temperature glides as its low critical temperature of 31.3 °C results in trans- or supercritical operation for higher-temperature applications [4]. Hydrocarbons on the other hand, are highly flammable and thus require significant safety precautions for safe operation [5].

Despite its challenges, water (R-718) has been identified as a suitable refrigerant to fill this gap. However, its high normal boiling point (100 °C) may result in sub-atmospheric pressures, high pressure ratios and low volumetric heating capacities. In addition, its high critical pressure (220.6 bar) may result in a high compressor discharge temperature causing technical problems [4]. It has been shown theoretically that mixing ammonia with water could solve the challenges related to the high water normal boiling point [6]. The high compressor discharge temperature on the other hand could be avoided by using compressor cooling, refrigerant injection and two-phase compression [4].

A HTHP demonstrator using water-ammonia mixture is currently being commissioned at Ghent University to experimentally demonstrate these solutions [4]. This contribution presents a dynamic model of this setup, allowing to do a detailed study of the system performance and control. In particular, the optimization of the liquid injection rate and bearing lubrication loop pressure are studied and the potential impact of the currently unknown bearing leakage is investigated to support the commissioning efforts. A brief description of the experimental demonstrator and the modelling approach are presented in Section 2. The results are shown and discussed in Section 3.

2. Methodology

2.1. Demonstrator

The demonstrator was designed for a heat sink inlet and outlet temperature of 170 and 200 °C, respectively. The envisaged heat source has an inlet temperature of 120 °C and temperature glide of 20 °C. The compressor drive power is 30 kW. Based on these specifications, a zeotropic water (86.5 mol%)-ammonia (13.5 mol%) mixture was selected based on detailed thermodynamic analysis and an experimental setup was designed [4]. Remark this mixture is highly zeotropic to match the high nominal temperature glide of 30 °C in the heat sink. A simplified schematic of the setup is shown in Figure 1. Only a short description of the setup is given in this contribution. More information on the design and rationale behind it can be found in [4, 7]. The design consists of the basic heat pump cycle extended with two additional loops, the 'bearing lubrication loop' (olive) and the 'two-phase injection loop' (orange).

The base cycle consist of the evaporator, compressor, condenser, liquid receiver and expansion valve. The most noticeable design choice is the oil-free twin-screw compressor. As mentioned above, compression of a water-ammonia mixture results in high discharge temperatures, which can cause high thermal stresses and jamming of the compressor. These elevated discharge temperatures can be avoided by liquid-injection in the compressor. Therefore, a twin-screw compressor has been selected as these are more tolerant to liquid carryover than reciprocating and centrifugal compressors. Twin-screw compressors are typically oil-lubricated to prevent component wear, to reduce leakage paths and to help with heat dissipation. However, these lubrication oils thermally degrade at high discharge temperatures. An oil-free design is thus used. The aforementioned beneficial effects of the oil can then be obtained by injecting liquid (or two-phase) working fluid into the compressor and more advanced sealing systems.

The 'bearing lubrication loop' (olive) circulates subcooled working fluid in the high- and low-pressure hydrodynamic bearings of the compressor. As indicated by the blue arrows on the figure, part of this lubricating flow inevitably leaks into the compressor. Leakage flow in the low-pressure bearing leaks to the compressor inlet, while flow from the high-pressure bearing leaks at intermediate pressure. The lubrication loop is not closed completely, and thus connected to the main heat pump loop to compensate for the leakage. Saturated liquid from the liquid receiver is expanded and subcooled in the subcooler fed by the heat source to ensure subcooled lubrication liquid.

While bearing leakage provides a cooling effect, the rate is not known a priori as it depends on unknown factors like sealing and tolerances. An additional 'two-phase injection control loop' (orange) is thus added to provide additional cooling. The injection loop is fed by expanding saturated liquid from the liquid receiver. The two-phase mixture is then mixed into the main flow after the evaporator, which allows to control the compressor inlet conditions in the two-phase region. Such two-phase injection is commonly referred to as liquid injection and this terminology is followed in this paper.

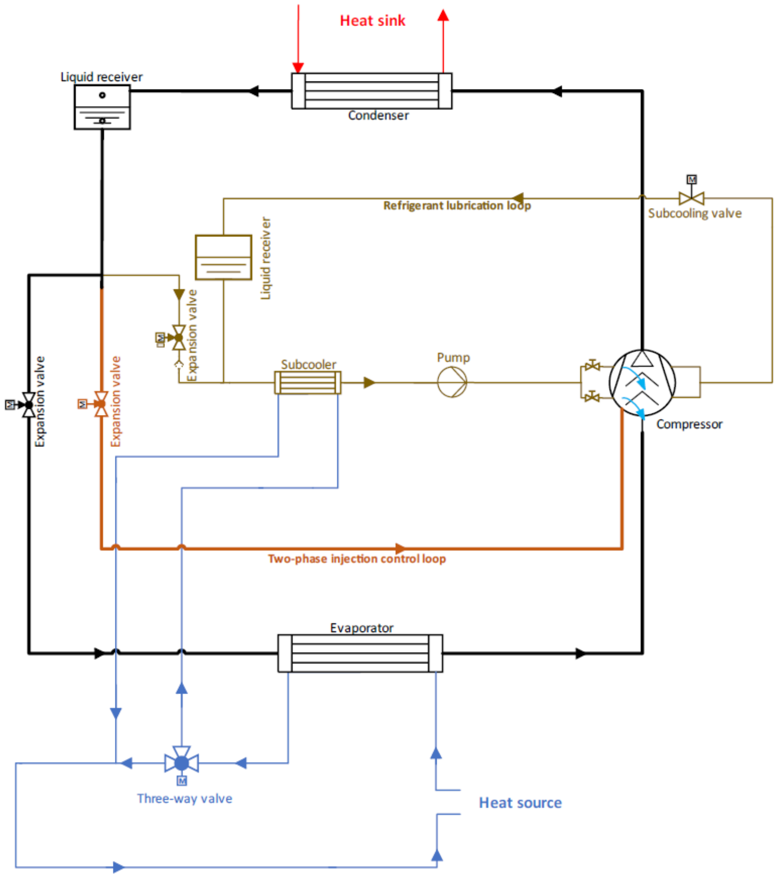

Figure 1. Simplified lay-out of the HTHP demonstrator [4].

2.2. Modelling approach

At the commissioning stage, the leakage rate of the compressor lubrication circuit is not known. A dynamic model of the system is made to develop a control strategy for the liquid injection and lubrication loop, and to verify that this control method is robust at different leakage rates. This dynamic model was programmed in the object-oriented modelling language Modelica [8], using Dymola 2022 [9] and the TIL-library 3.14.0 [10]. Component models from this library were used, and extended when necessary.

2.2.1. Heat exchangers

The main loop includes two counterflow heat exchangers (HEX). The condenser is a plate-and-shell HEX, while the evaporator is a plate heat exchanger. The finite volume plate heat exchanger model of the TIL-library [10] is used to model both, as it has been shown in literature to sufficiently capture the behavior of a plate-and-shell HEX [11]. SWEP-geometries were used [12]. The detailed geometry and explanation on the selection procedure is given in [13]. The discretized TIL-model considers the convection at both wall sides and the conduction through it. On the refrigerant side, a constant heat transfer coefficient has been assumed for each phase. An approximate value of 6260 W/(m² K) was used for the two-phase heat transfer [14]. Based on this value, the heat transfer coefficients in the liquid and vapor phase were approximated as 45% [15] and 25% [16] of the two-phase value, respectively. The thermal oil in the heat source and sink remains liquid. A constant convection coefficient of 815 W/(m² K) [14] has thus been assumed over the full HEX length. Finally, all pressure drops in the heat exchangers were assumed proportional to the quadratic mass flow [11]. The nominal mass flow and pressure drop were obtained from the manufacturer [14].

2.2.2. Twin-screw compressor

The twin-screw compressor is based on the physics-based scroll compressor model in the TIL-library, as a screw compressor was not available in TIL 3.14.0 [10]. The semi-empirical model is based on the conservation laws of mass, energy and momentum, complemented by empirical parameters. Key empirical parameters of the model include pressure drops at the suction and discharge ports, internal leakage, friction and heat losses. In addition to the main compression, the liquid injection and bearing leakage paths must be included. A schematic of the extended twin-screw compressor is shown in Figure 2. In the figure, the black blocks represent the structure of the available scroll compressor model in the TIL-library, while the green lines and arrows represent added parts. The liquid injection and low-pressure bearing leakage are modelled as fluid injections upstream of the compressor. The high-pressure side bearings are in contact with multiple working chambers at different pressures, and they thus leak at intermediate pressure. As the base TIL-model does not allow for injection at intermediate pressure, two base TIL-models were connected in series and the model parameters were adjusted according to the combined structure. A complete description of all calculations and numerical values is provided in [13]. Here, focus is given to the global approach.

Splitting the compressor in two submodels requires adaptation of each built-in volume ratio. Both built-in volume ratios were chosen as the square root of the built-in volume ratio of the complete compressor to mimic the behavior of a single compressor. The displacement volume of the second compressor model was corrected for the partial compression upstream using the built-in ratio of the first compressor. The pressure loss calculation for the suction- and discharge ports was updated too. The basic TIL-submodels calculate these pressure drops based on the Saint-Venant and Wantzel equation, often used for valves. Twin-screw compressors use ports, rather than valves, resulting in smaller pressure drops at the suction- and discharge port. The flow areas of the real suction and discharge port were confidential and could not be supplied by the manufacturer. Therefore, they were selected according to [17], who investigated a twin-screw compressor with similar built-in volume ratio and swept volume. The pressure drop at the discharge side of the first and suction side of the second submodel are introduced by the modelling approach and are not present in the actual compressor. Therefore, these non-existing ports are given large dimensions which results in negligible pressure drops. Each TIL-compressor also contains a leakage path between the discharge and suction volume. These separate paths were replaced by one leakage path between the discharge and suction of the complete compressor. The corresponding leakage area was set according to [18]. The leakage area in the submodels was set to a small value, ensuring that the mass flow through these paths remained below 1% of the compressor flow rate, while avoiding numerical instability. Heat loss from the compressor mainly occurs at the discharge side. Therefore, the heat loss coefficients of the first compressor volumes were set to zero, while the heat loss coefficient of the final volume was determined according to [18]. The friction losses are calculated following the original approach of the TIL-library, but only accounted for in the first submodel. The empirical coefficients were determined assuming a mechanical efficiency of 95% in the nominal operating point [19]. As mentioned before, the liquid injection and low-pressure side bearing leakage are assumed to occur in the suction line, before the first compressor block. The high-pressure side leakage is geometrically implemented in between both compressor blocks. A first estimate for the leakage area of both valves was made based on a similar compressor in [20], and its impact is verified in the Section 3.3.

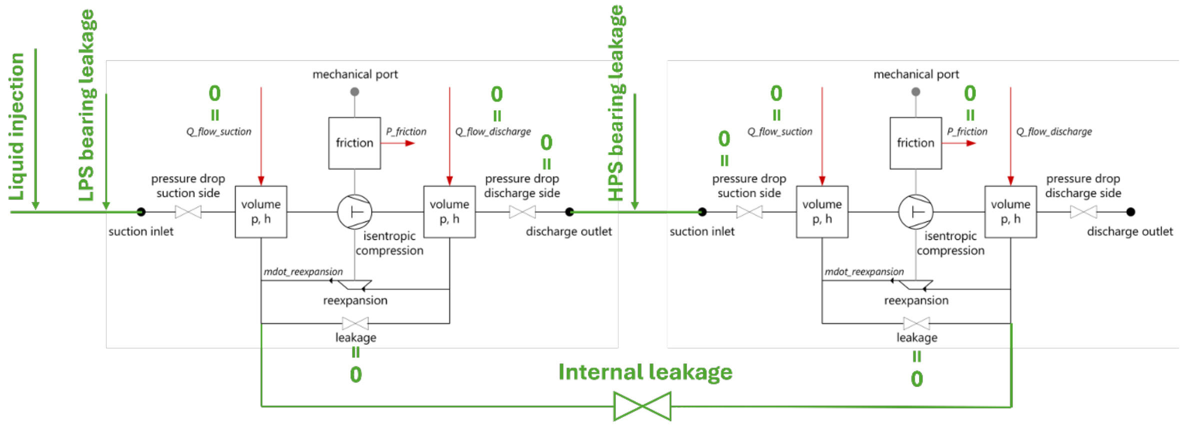

Figure 2. Twin-screw compressor model with liquid injection and bearing leakage extended from [10].

2.2.3. Other components

The other components are modelled using the standard components of the TIL-library [10]. The expansion valves are modelled using the orifice valve model, which calculates the mass flow rate as function of the pressure drop across the valve using the Bernouilli-equation. A high-pressure reservoir is present in the cycle as it extends the part-load range by buffering the varying refrigerant charge in the heat exchangers under different operating conditions [21, 22]. The ideal separator model of the TIL-library was used, assuming equilibrium conditions at the outlet. The pumps in the secondary circuit are modelled using the second-order pump model of the library. The subcooler of the refrigerant lubrication loop shown in Figure 1 is modelled simply by using the TIL-tube model, with a fixed 5 K subcooling implemented via heat extraction. While more detailed components could be implemented, this approach results in similar thermodynamics with reduced model complexity.

2.2.4. Cycle modelling

The component models are combined to make the full cycle model shown in Figure 3. Note that the lay-out is slightly simplified compared to the demonstrator shown in Figure 1. The lubrication loop (olive in Figure 1) is not modelled completely. Instead, it is represented by a main expansion valve controlling the pressure of the lubrication branch, the simplified subcooler (see Section 2.2.3.) and two expansion valves representing the leakage from the bearings to the compressor chambers. These two valves thus correspond to the modelling of the compressor leakage areas (see Section 2.2.2) rather than the flow control valves of the lubrication loop as represented in Figure 1. The leakage refrigerant evaporates inside the compressor, enhancing cooling, while losses are compensated directly from the main loop. This approach captures the main thermodynamic effects with a simpler model lay-out.

The two-phase injection loop (orange in Figure 1) is modelled similar to the real demonstrator. It taps refrigerant from the high-pressure side of the HTHP and injects it into the low-pressure line. The injection rate can be controlled by adapting the throughflow area of the expansion valve to influence the discharge temperature (see Section 2.3).

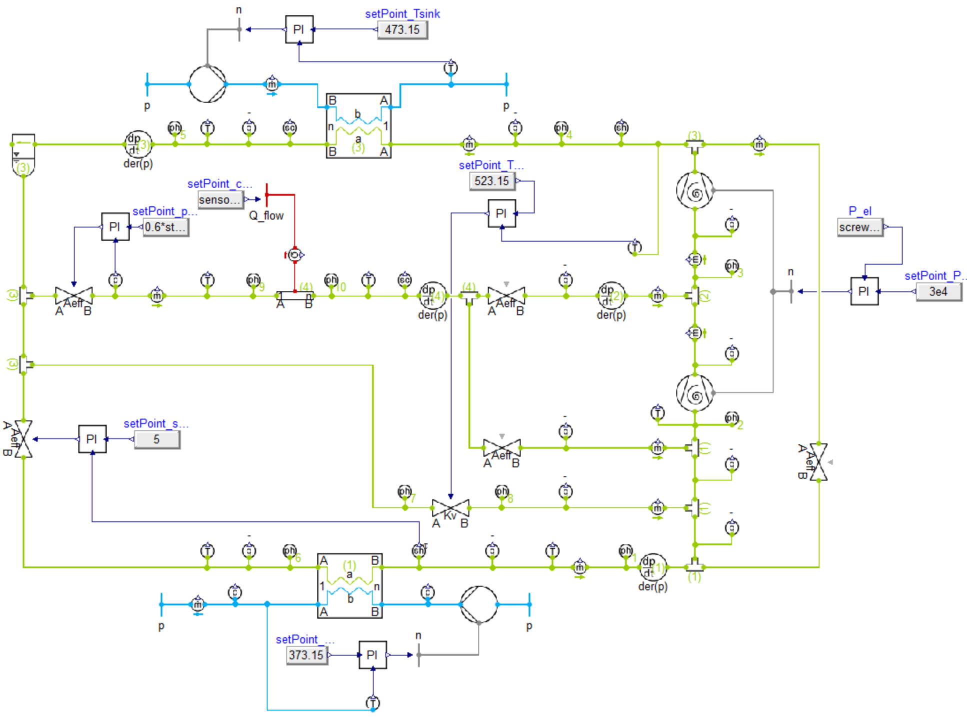

Figure 3. Simplified representation of the model layout.

2.3. Controller design

Key parameters are controlled by adjusting the corresponding manipulated variables using PI-controllers, as shown in Figure 3. In nominal operation, the heat source and sink temperatures are kept constant, allowing fair comparison of the COP in between cases. The heat source and sink pump speeds are controlled to maintain the respective outlet temperatures at their nominal values of 100 °C and 200 °C. The nominal drive power is 30 kW. Variable-speed control of the compressor has proven effective to modulate the power uptake [23]. A first PI-controller thus adjust this speed depending on the instantaneous power uptake to keep it constant at its nominal value. As the operating point is determined mainly by the intersection of the compressor and valve characteristic, a change in compressor speed influences the pressure levels in the cycle. Therefore, a second PI-controller controls the effective throughflow area of the expansion valve to maintain a suitable superheat level of 5 °C at the evaporator outlet. The leakage areas of the bearings cannot be controlled, as they model a geometrically defined phenomenon. However, the valve connecting the lubrication branch with the main loop is controlled to keep the lubrication pressure constant, targeting 60% of the condenser pressure in nominal conditions to satisfy the operational constraints dictated by the compressor internal components. The valve throughflow area is controlled based on the difference between the measured and desired lubrication pressure. Finally, the liquid injection rate is controlled by adjusting the valve k_v-value (and thus effective throughflow area) with another PI-controller based on the compressor discharge temperature, aiming to keep it at its maximum value of 250 °C. A detailed description of the control structures, tuning parameters and output limits can be found in [13].

2.4. Test conditions

This contribution supports the ongoing development of the HTHP-demonstrator. At this commissioning stage, the model's primary purpose is to gather insight in the global system behavior and the effectiveness of the control structure. After verification of the model energy balance and capability to reach nominal conditions, a sensitivity study to the main setup novelties was conducted. In particular, the influence of the liquid injection rate, pressure of the bearing lubrication loop, and bearing leakage rate was of interest.

The liquid injection rate and pressure of the bearing lubrication loop are controlled in nominal conditions to maintain a compressor discharge temperature of 250 °C and lubrication loop pressure equal to 60% of the condenser pressure in nominal conditions, respectively. To test the influence of these parameters in realistic conditions, the respective PI-controller is disabled and the manipulated variable is manually varied. The manipulated variable is initialized on its nominal value, and then slowly ramped to a new steady value to verify its impact. This procedure has been repeated for different end values to cover a representative sensitivity range.

The bearing leakage rate on the other hand depends on the confidential compressor geometry and is thus uncertain. The need for liquid-injection and the effectiveness of the proposed control structure is thus not known. While it is informative to explore the effect of reduced leakage, the main objective is to examine how increased leakage would affect system performance. As explained in Section 2.2.2, the low-pressure and high-pressure leakage are modelled with respective valves and their throughflow area was estimated based on literature. Due to the bearing symmetry, an identical gap was assumed for the high-pressure and low-pressure side bearing. This leakage area has been varied in a relevant sensitivity range while keeping the other parameters constant and all PI-controllers active. As such the impact of this leakage gap on the nominal operation can be assessed.

3. Results and discussion

3.1. Liquid injection rate

Liquid injection is implemented to avoid excessive compressor discharge temperatures, while maintaining good efficiency. In nominal conditions, the injection valve k_v- value (and thus area) is controlled to maintain the design value of 250 °C. In Figure 4, the impact of the k_v- value and thus liquid injection rate on the compressor discharge temperature and coefficient of performance (COP) are visualized. The figure clearly shows that liquid injection can effectively control the compressor discharge temperature. The discharge temperature reduces with increasing k_v- value, and thus injection rate, until it reaches a plateau when the compressor outlet enters the two-phase region. Reducing the k_v- value compared to its nominal value increases the outlet temperature, as expected. Without injection, the discharge temperature reaches up to 360 °C which illustrates the injection need. The COP shows a more complex evolution. Starting without injection ($k_v = 0$), the COP initially rises due to the more isothermal compression. However, it peaks at an injection rate of 0.0021 kg/s, beyond which it decreases. Remark that the discharge temperature at optimal efficiency exceeds the allowable compressor discharge temperature limit of 250 °C, which means it cannot be used in practice. All feasible operating points lie right of the nominal injection, meaning it is practically beneficial to minimize the injection to keep the discharge temperature just below the allowable limit. The overall evolution of the COP curve can be attributed to the competing effects described in the PhD thesis of Vieren [7]. First, the compression more closely approaches the isothermal ideal as the discharge temperature decreases. However, a lower discharge temperature also means less heat is transferred to the sink during desuperheating. In traditional vapour compression cycles, the pinch point typically occurs at the saturated vapour point and gradually shifts more to the heat sink outlet with lower compressor outlet temperatures. This means a higher condenser pressure is thus required to maintain a similar pinch point temperature difference and thus heat transfer, leading to higher specific compression work. A similar effect can be observed in the current simulations, even though the significant refrigerant glide in the two-phase region and that the pinch point is not fixed as was done by Vieren [7]. Without liquid injection, the pinch point is located at the saturated condenser outlet as the heat exchanger is effectively oversized due to the high heat transfer in the superheated region, which is caused by the high compressor outlet temperature and thus high local driving temperature difference. With increased liquid injection, the effect observed by Vieren [7] becomes visible. The compressor outlet temperature and heat transfer in the superheated region decrease. Consequently, the pinch point shifts to the saturated vapour point and moves towards the condenser inlet with increasing injection. The condenser pressure indeed increases with decreasing superheat at the condenser outlet to maintain a sufficiently high driving temperature difference. As the power uptake of the compressor is controlled at 30 kW, the sink heat transfer thus reduces which results in decreasing COP values for high injection rates. It can be seen that the decrease in COP becomes less steep at an injection rate of 0.0084 kg/s, which corresponds to the point where the discharge enters the two-phase region. As the saturation temperature and thus the heat sink temperature difference stabilize, the pressure remains more constant. Still, it increases slightly due to the decreasing enthalpy difference across the condenser which explains the continued decrease in COP.

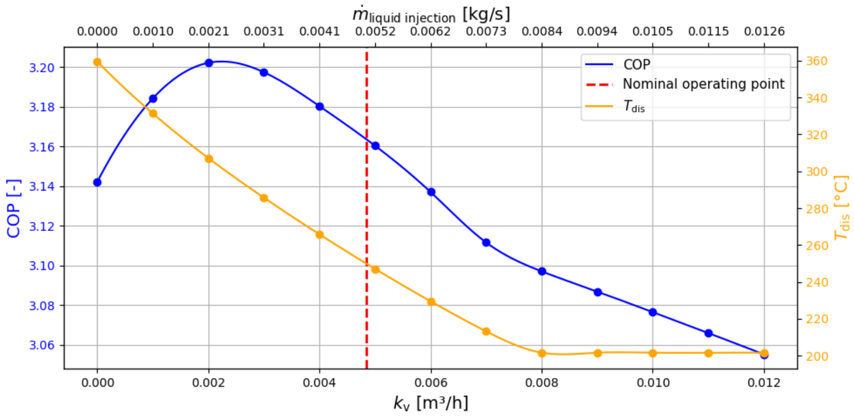

Figure 4. Coefficient of performance COP (left axis) and compressor discharge temperature T_{dis} (right axis) as a function of the injection valve k_v-value and liquid injection mass flow rate.

3.2. Pressure of the bearing lubrication loop

The bearing loop pressure can be controlled actively. Figure 5 shows the impact of this pressure on the cycle COP by a sensitivity study around its nominal value of 60% of the condenser pressure. The compressor discharge temperature is omitted, as it is kept at its nominal value of 250 °C for all pressures by the active control. It can be seen that the COP increases with increasing bearing loop pressure. However, the increase remains smaller than 1% over the full range. The HTHP is thus rather insensitive to this injection pressure, which means that precise tuning and optimization is not critical.

The COP increase can mainly be attributed to the operation of the subcooler. The heat transfer in the subcooler depends on the leakage mass flow rate in the lubrication branch $\dot{m}_{leak}$, and the enthalpy difference $\Delta h_{subcooler}$ corresponding to 5 °C subcooling across it. Both are shown in Figure 6 as function of the bearing loop pressure. The leakage flow in the bearings increases with increasing bearing lubrication loop pressure, but $\Delta h_{subcooler}$ reduces. The subcooler inlet enthalpy depends on the main refrigerant loop and remains nearly constant, while the outlet temperature and outlet enthalpy increase with increasing pressure due to the higher saturation temperature and constant 5 °C subcooling. At low pressures, the increased mass flow dominates the reduced enthalpy difference and the subcooler heat transfer rate increases, which results in more effective compressor cooling. In turn, this reduces the required liquid injection, allowing more refrigerant to pass through the evaporator. This increases the heat input and slightly improves the COP. Around a lubrication pressure of 7 bar, the subcooler cooling rate reaches a maximum and starts decreasing as the $\Delta h_{subcooler}$ drops sharply. The bearing leakage thus cools the compressor less effectively, and the liquid injection increases to maintain the desired discharge temperature. This increased injection slightly decreases the heat uptake in the evaporator. However, this decrease is minor compared to the substantial drop in subcooler heat rejection, and the condenser heat rejection and system COP continue to increase.

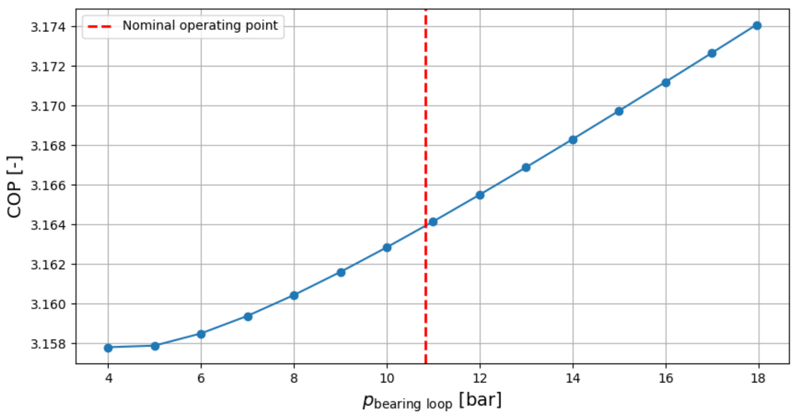

Figure 5. Impact of the bearing lubrication loop pressure on the COP.

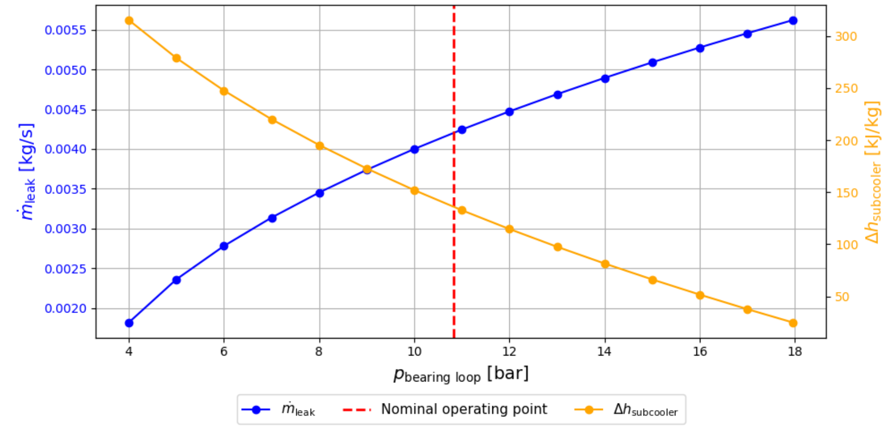

Figure 6. Leakage mass flow rate $\dot{m}_{leak}$ (left axis) and enthalpy difference across the subcooler $\Delta h_{subcooler}$ (right axis) as function of the bearing lubrication loop pressure $p_{bearing\ loop}$.

3.3. Bearing leakage area

The bearing leakage area is currently uncertain. Therefore, it is important to assess the performance sensitivity to this parameter despite it not being controllable. The leakage area has been varied, resulting in varying leakage mass flow rate. The impact on the COP and liquid injection required is shown in Figure 7. Initially, a slight increase in COP is observed. In this region, the liquid injection rate decreases with increasing leakage rate as the discharge temperature is actively controlled at 250 °C. This initial small COP improvement is attributed to the more effective cooling provided by the subcooled refrigerant into the compressor, compared to the liquid injection at the inlet. However, this difference is insignificant as the rise is less than 0.2%.

Beyond a leakage mass flow rate of 0.088 kg/s, the COP begins to decrease. At this point, liquid injection is reduced to zero and cannot further decrease to compensate for the increased leakage. Consequently, the total cooling flow increases and the discharge temperature cannot be maintained at 250 °C. This excess cooling leads to a performance drop similar to the trend observed in the liquid injection flow rate analysis (see Section 3.1).

The sensitivity analysis thus reveals bearing leakage has minimal effect on the HTHP performance near the nominal operation point (red dotted line in Figure 7), but excessive leakage beyond expected levels can significantly reduce system performance.

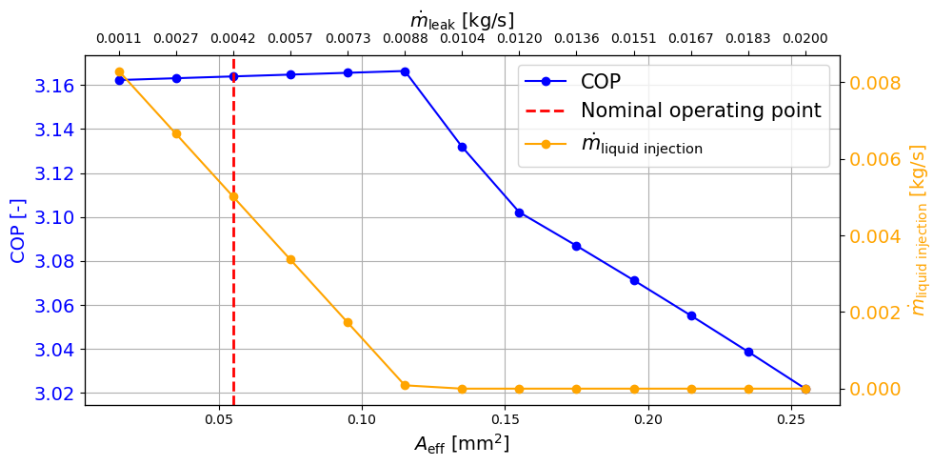

Figure 7. COP (left axis) and liquid injection rate (right axis) as function of the bearing leakage area A_{eff} and leakage flow rate $\dot{m}_{leak}$.

4. Conclusion

This contribution numerically assessed the expected effects of liquid injection, lubrication loop pressure and bearing leakage on HTHP performance to support the setup commissioning and development of liquid injected HTHPs. First, it proposed a feasible control strategy for nominal operation. It then assessed the performance sensitivity on the parameters of interest. Among them, liquid injection was shown to have the most significant influence. However, the COP peaked at an injection rate exceeding the thermal limits of the compressor. In practice, it is thus beneficial to minimize the liquid injection to keep the compressor discharge temperature at its maximum allowable value. For the current demonstrator, this maximum temperature was determined as 250 °C and a COP of 3.16 was calculated. The influence of the bearing lubrication loop pressure was shown to be negligible in the studied range, which means that precise tuning and optimization is not critical for the heat pump operation. Finally, the sensitivity to the uncontrollable and uncertain bearing leakage was verified. It was shown that bearing leakage variations in the expected range have only limited effect on the performance, as the liquid injection rate can be adapted accordingly. However, excessive leakage can lead to efficiency loss and should be addressed through seal optimization. Future work will first focus on experimental validation and calibration of the model once the setup commissioning is finalized. Moreover, the compressor and leakage modelling will be further refined based on the experimental results. The improved model will then be used to examine and optimize the system control in typical industrial transient and off-design conditions.

References

[1] Ritchie H. Sector by sector: where do global greenhouse gas emissions come from? [Internet]. Our World in Data. [cited 2025 Nov 11]. Available from: https://ourworldindata.org/ghg-emissions-by-sector
[2] de Boer R, Andrew M, Zühlsdorf B, Arpagaus C, Bantle M, Wilk V, Elmegaard B, Corberán-Salvador, JM, Benson J. Strengthening Industrial Heat Pump Innovation: Decarbonizing Industrial Heat. 2020.
[3] Zühlsdorf B, Poulsen JL, Dusek S, Wilk V, Krämer J, Rieberer R, Verdnik M, Demeester T, Vieren E, Magni C, Abedini H, Leroy C, Yang L, Andersen MP, Elmegaard B, Turunen-Saaresti T, Uusitalo A, De Carlan F, Gachot C, Schlosser F, Klöppel S, Khass OA, Schaffrath R, Wittstadt U, Henninger S, Teles de Oliveira H, Kaida T, Ramirez M, Lycklama a Nijeholt JA, Schlemminger C, Moen OM, Lee G, Arpagaus C. Annex 58 High-Temperature Heat Pumps Task 1 - Technologies. 2023.
[4] Vieren, E., Couvreur, K., De Paepe, M., Lecompte, S., 2024. "Design of a high-temperature heat pump providing heat up to 200 °C," 16th IRR Gustav Lorentzen Conference on Natural Refrigerants. Maryland, USA, paper # 1229.
[5] Harby K. Hydrocarbons and their mixtures as alternatives to environmental unfriendly halogenated refrigerants: An updated review. *RSER* 2017;**73**:1247-1264.
[6] Vieren E, Demeester T, Beyne W, Andersen MP, Elmegaard B, Arteconi A, De Paepe M, Lecompte S. Selection of pure and binary working fluids for high-temperature heat pumps: A financial approach. *Appl. Therm. Eng.* 2024;**252**:123615.
[7] Vieren E. Advancing Industrial High-Temperature Heat Pumps trough Financial, Thermodynamic and Technological Evaluation. 2025.
[8] Modelica and the Modelica Standard Library [Internet]. 2023. [cited 2023 Nov 22]. Available from: https://modelica.org/
[9] Dymola 2022 [Internet]. 2022. [cited 2023 Nov 22]. Available from: https://www.3ds.com/products-services/catia/products/dymola/
[10] TIL Suite - The library for thermodynamic systems [Internet]. 2023. [cited 2023 Nov 22]. Available from: https://tlk-energy.de/en/software/til-suite
[11] Meesenburg W, Markussen WB, Ommen T, Elmegaard B. Optimizing control of two-stage ammonia heat pump for fast regulation of power uptake. *Appl. Energy* 2020; **271**:115126.
[12] SWEP. SWEP - products [Internet]. SWEP. [cited 2023 Nov 22]. Available from: https://www.swep.net/products/
[13] Huyghe T. Numerical investigation of bearing leakage and liquid injection in industrial high temperature heat pumps. 2025. (MSc thesis Ghent University)
[14] SWEP SSP G8 [Internet]. 2024. [cited 2023 Nov 22]. Available from: https://desktop helpfile.swep.net/#/
[15] Kharangate CR, O'Neill LE, Mudawar I, Hasan MM, Nahra HK, Balusubramaniam R, Hall NR, Macner AM, Mackey JR. Effects of subcooling and two-phase inlet on flow boiling heat transfer and critical heat

flux in a horizontal channel with one-sided and double-sided heating. *Int. J. Heat Mass Transf.* 2015;**91**:1187-1205.

[16] Zhang L, Liu J, Xiongwen X. Numerical simulation of heat transfer performance of R410A in condensing-superheated zone. *IJR* 2021;**128**: 206-217.

[17] Williams TL. Investigation into the performance of a twin-screw compressor for helium compression. 2022. (PhD thesis Michigan State University)

[18] Guiffrida A, A semi-emperical method for assessing the performance of an open-drive screw refrigeration compressor. *Appl. Therm. Eng.* 2016;**93**:813-823.

[19] Markovich DM, Ermakov A, Salakhov R, Khismatullin R, Alexeenko SV, Morozov AA. Improving the performance of vapor compression cycle using an internal heat exchanger. *E3S Web Conf.* 2023;**459**:07003.

[20] Chuang W, Xing Z, Pan X, Zhilong H. Simulation of the characteristics of the water-lubricated journal bearing in twin-screw air compressor. *ILT* 2018;**70**:1476-1486.

[21] Pomme, V., 1999. "Improved Automotive A/C Systems Using a New Forced Subcooling Technique," SAE International Congress and Exposition. Warrendale, USA, paper #1192.

[22] Andritos, G., Desideri, A., Gantiez, C., Lemort, V., Quolin, S., 2016. "Steady state and dynamic modelling of a 1 MWel commercial waste heat recovery ORC power plant," 29th International Conference on Efficiency, Cost, Optimisation, Simulation and Environmental Impact of Energy Systems. Portoroz, Slovenia.

[23] Tassenoy R, Laterre A, Lemort V, Contino F, De Paepe M, Lecompte S. Assessing the influence of compressor inertia on the dynamic performance of large-scale vapor compression heat pumps for Carnot batteries. *J. Energy Storage* 2024;**101**:113948.